NAVAL POSTGRADUATE SCHOOL
Monterey, California

THESIS

AN EXPERIMENTAL INVESTIGATION OF THE EFFECTS OF
SWIRLING AIR FLOWS ON THE COMBUSTION PROPERTIES
OF A SOLID FUEL RAMJET MOTOR

by

William H. Campbell, Jr.

September 1985

Thesis Advisor: David W. Netzer

REPORT DOCUMENTATION PAGE		READ INSTRUCTIONS BEFORE COMPLETING FORM
1. REPORT NUMBER	2. GOVT ACCESSION NO.	3. RECIPIENT'S CATALOG NUMBER
4. TITLE (and Subtitle) An Experimental Investigation of the Effects of Swirling Air FLows on the Combustion Properties of a Solid Fuel Ramjet Motor		5. TYPE OF REPORT & PERIOD COVERED Master's Thesis September 1985
		6. PERFORMING ORG. REPORT NUMBER
7. AUTHOR(s) William H. Campbell, Jr.		8. CONTRACT OR GRANT NUMBER(s)
9. PERFORMING ORGANIZATION NAME AND ADDRESS Naval Postgraduate School Monterey, California 93943-5100		10. PROGRAM ELEMENT, PROJECT, TASK AREA & WORK UNIT NUMBERS N0001985WR51139
11. CONTROLLING OFFICE NAME AND ADDRESS Naval Weapons Center China Lake, California 93555		12. REPORT DATE September 1985
		13. NUMBER OF PAGES 70
14. MONITORING AGENCY NAME & ADDRESS(if different from Controlling Office)		15. SECURITY CLASS. (of this report) Unclassified
		15a. DECLASSIFICATION/DOWNGRADING SCHEDULE

16. DISTRIBUTION STATEMENT (of this Report)

Approved for public release; Distribution is unlimited

17. DISTRIBUTION STATEMENT (of the abstract entered in Block 20, if different from Report)

18. SUPPLEMENTARY NOTES

19. KEY WORDS (Continue on reverse side if necessary and identify by block number)

Solid Fuel Ramjet, Swirling Airflows, Regression rate, Swirl Number
Tube-in-hole injector

20. ABSTRACT (Continue on reverse side if necessary and identify by block number)

A series of reacting flow tests of a solid fuel ramjet were conducted with different air inlet swirl. Cold flow measurements of the air flow at the exit plane of the tube-in-hole injector were used to determine the Swirl Number for each configuration. Regression rates of the HTPB fuel at low air mass flux were found to increase with swirl vane angle (and Swirl Number) up to 30 degrees.

DD FORM 1473 EDITION OF 1 NOV 65 IS OBSOLETE
1 JAN 73

S N 0102-LF-014-6601

1

An Experimental Investigation of the Effects of
Swirling Air Flows on the Combustion Properties
of a Solid Fuel Ramjet Motor

by

William H. Campbell, Jr.
Lieutenant, United States Navy
B.S., University of Mississippi, 1978

Submitted in partial fulfillment of the
requirements for the degree of

MASTER OF SCIENCE IN AERONAUTICAL ENGINEERING

from the

NAVAL POSTGRADUATE SCHOOL
September, 1985

ABSTRACT

A series of reacting flow tests of a solid fuel ramjet were conducted with different air inlet swirl. Cold flow measurements of the air flow at the exit plane of the tube-in-hole injector were used to determine the Swirl Number for each configuration. Regression rates of an HTPB type fuel at low air mass flux were found to increase with swirl vane angle (and Swirl Number) up to 30 degrees.

TABLE OF CONTENTS

4

LIST OF TABLES

LIST OF FIGURES

TABLE OF SYMBOLS

Ath   = effective throat area

Cd   = nozzle discharge coefficient

di   = initial port diameter

df   = final port diameter

Dp   = fuel grain port diameter

Dth   = nozzle throat diameterure

$\overline{F}$ = average thrust

F   = thrust

f   = final, fuel

γ = ratio of specific heats

G   = mass flow per unit area in the fuel port,
              ratio of maximum swirl to axial velocities

G_θ = tangential flux of momentum

G_x = axial flux of momentum

i   = initial, inlet

L   = length of solid fuel grain

$\dot{m}$ = mass flow rate

Pa   = air sonic choke pressure, chamber pressure
              0.2 secs. before ingnition

$\overline{Pc}$ = combustion chamber pressure

Pc   = average combustion chamber pressure

Ph   = motor head-end pressure

Phf   = heater fuel sonic choke pressure

7

TABLE OF SYMBOLS
(cont'd)

Pho	=	heater oxidizer sonic choke pressure
Pif	=	ignition fuel sonic choke pressure
Pt	=	stagnation pressure
R	=	gas constant
$\dot{r}$	=	regression rate
f	=	density of fuel
S	=	Swirl NUmber
S(avg)	=	mass averaged Swirl Number
ta	=	air time
tb	=	burn time
ti	=	ignition time
Ti	=	inlet air temperature
$\overline{Ti}$	=	average inlet air temperature
tp	=	purge time
Tt	=	stagnation temperature
u	=	axial velocity
u(avg)	=	average axial velocity
u(max)	=	maximum axial velocity
u(outer)	=	axial velocity of flow between inlet wall and tube-in-hole injector
w	=	tangential velocity
w(avg)	=	average tangential velocity
w(max)	=	maximum tangential velocity
$\triangle$ W	=	change in weight of fuel grain during run

ACKNOWLEDGEMENT

I. INTRODUCTION

A. SOLID FUEL RAMJET

Ramjet technology has taken three distinct approaches to meet the requirements of an ever-expanding mission responsibility "placed upon weapon systems of today. These three concepts are the Liquid Fuel Ramjet (LFRJ), Solid Fuel Ramjet (SFRJ) and the Ducted Rocket (DR). Each system has distinct advantages over the other. The LFRJ has the capability to operate over widely different levels of thrust and efficiency through use of variable fuel control. The SFRJ is lighter, more compact, and is much less complex than the LFRJ due to the absence of fuel tanks, fuel delivery and control mechanisms. The DR retains some of the benefits of the SFRJ, but must carry oxidizing materials within the fuel to maintain combustion.

Because of the simplicity with which the SFRJ operates, and its relative compactness, it is desireable to develop a simple thrust control for the solid fuel ramjet motor. To understand how this problem may be approached, it is first necessary to have a working knowledge of the basics of ramjet technology.

As stated earlier, the ramjet is a very simple engine. Since there is no compressor, the ramjet uses supersonic velocities to compress the air flow. Figure 1 depicts the

10
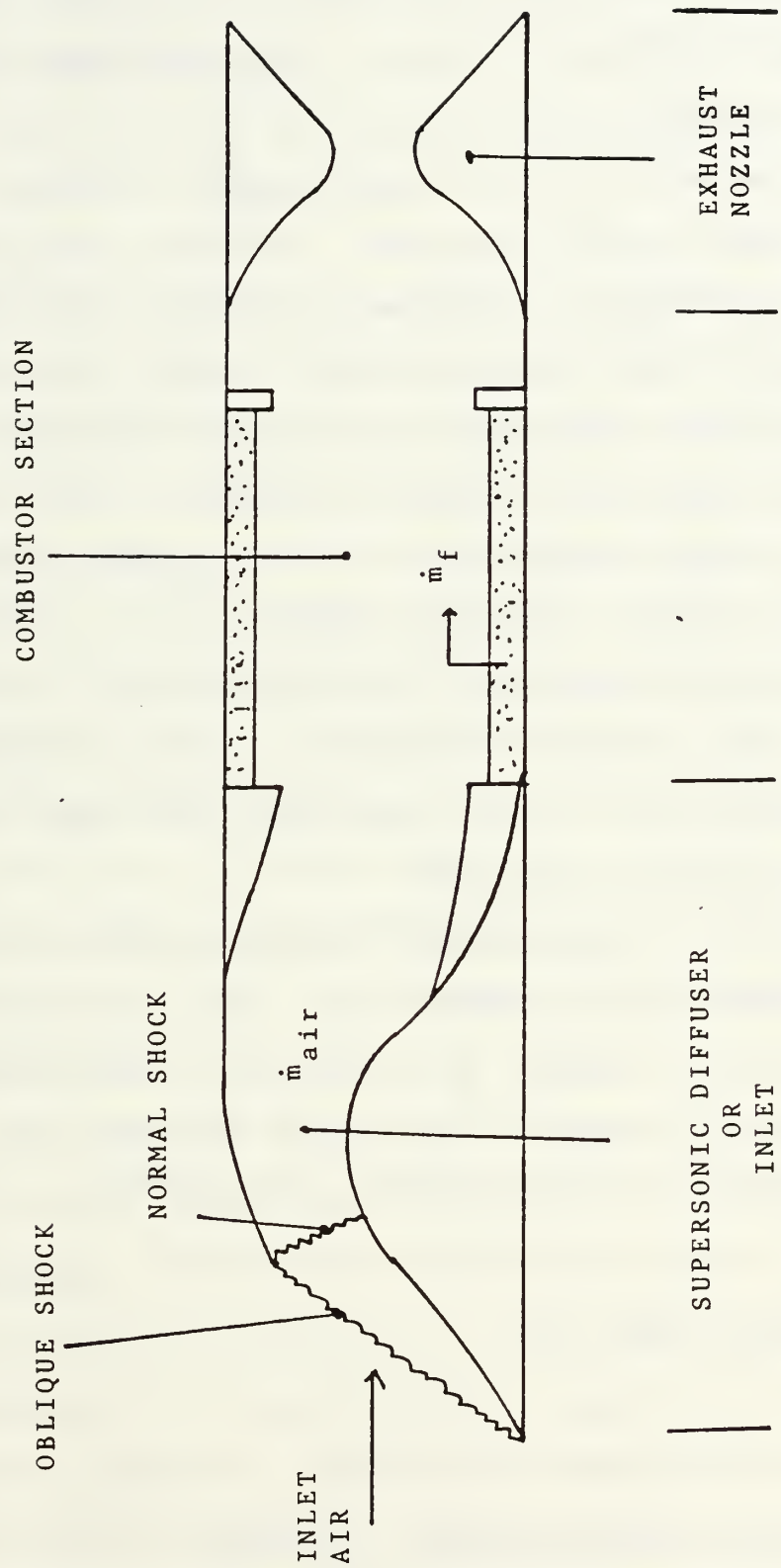
Figure 1. Schematic of Simple SFRJ

11

basic SFRJ. The three components of the basic SFRJ are the supersonic diffuser or inlet, the combustor, and the exhaust nozzle.

As supersonic flows enter the SFRJ diffuser, several significant events take place. Standing shocks are present at the air inlet. An increase in static temperature and decrease in flow velocity occurs through the shock waves. Combustion of the solid fuel increases the mass flow slightly and the temperature is again increased. This larger mass flow at higher temperature is then expanded through the exhaust nozzle. A detailed description is given by United Technologies Corporation, Chemical Systems Division [Ref. 1]. It is the increase (or decrease) of the fuel prolysis rate or regression rate ($\dot{r}$) that determines the thrust and effects the efficiency of the SFRJ.

There are many methods that can be used to affect the regression rate of a solid fuel. One is to change the fuel composition. Another is to change the environmental effects on the fuel, such as the chamber pressure (Pc), inlet air temperature, and the mass flux through the port of the fuel grain. A typical regression rate formula is given by Boaz and Netzer [Ref. 2]

$$\dot{r} = c\ Pc^{0.51}\ \ G^{0.41}\ \ T^{0.38} \tag{1}$$

for motors not using bypass air where

12

c = constant

Pc = chamber pressure

G = mass flow per unit area in the fuel port

Ti = inlet air temperature

The SFRJ is self-throttling through the effect of G on $\dot{r}$. However, the self-throttling is not sufficient for many missions. Alternate means for varying $\dot{r}$ are therefore desired. Changing G can be accomplished by either changing $\dot{m}$ (such as in bypass designs) or by changing the flow area. Variable bypass is one possible means for controlling $\dot{r}$.

Ko [Ref. 3] investigated the effects of inlet air swirl on the regression rate of the solid fuel grain. Swirl imparts an angular component of mass flux into the flow field which can effect the residence time of the flow by increasing the effective length of the combusion section of the ramjet motor. It can also affect the convective heat transfer to the fuel surface and the mixing rates of fuel and oxygen. It was found that swirl may be an effective means for regression rate control, although only limited data were obtained.

B. SWIRL NUMBER

The introduction of swirl into a flow causes difficulty in characterization of the flow field. There is no longer only the axial component of the flow but now radial and tangential components as well. The Swirl Number (S) is one way to characterize the flow. Lilley and others [Ref. 4]

13

have done considerable work with swirling flows and have set
forth the non-dimensionalized swirl number (for specific
assumptions about the inlet swirl behavior) as

$$S = \frac{G_\theta}{G_x \, (d/2)} \qquad (2)$$

where

$\acute{G}_\theta$ = tangential flux of swirl momentum

G_x = axial flux of momentum

$d/2$ = equivalent inlet radius

This thesis investigated the effects of varying the inlet
air flow angle on the combustion process of a non-bypass
SFRJ. This was accomplished by using tube-in-hole injectors
with vanes of 0, 15, 30, and 45 degrees. Cold flow
measurements were made to determine inlet flow angles, and
reacting flow tests were conducted to determine the effects
on fuel regression rate.

II.   DESCRIPTION OF APPARATUS

A.   RAMJET MOTOR

The ramjet motor used in this investigation was identical with one used in earlier invesigations at he Naval Postgrátduate School [Refs. 2,3]. Figure 2 is a schematic of the head-end assembly, step insert section, fuel grain and nozzle.

The head-end assembly used a wedge to turn the primary inlet air from 90 degree plenum dumps. The igniter torch and and ignition gas were injected into the recirculation zone just aft of the step insert.

The step insert section acted as the air inlet, which was modified with a tube-in-hole injector. The step height allowed for sudden expansion of the flow into the combustion section as depicted in Figure 3. This sudden expansion allows a flame to be stabilize behind the step by creating a recirculation zone. The swirl elements and tube were fabricated from stainless steel. Each swirl blade was a cambered airfoil attached at the hub with silver solder. The vane tips were ground for minimum clearance at the tube inner wall, and then silver soldered along the downstream side of the blades. Figure 4 shows the tubes with the swirlers used in this experiment. Tubes with 15, 30, and 45 deg. (from

15
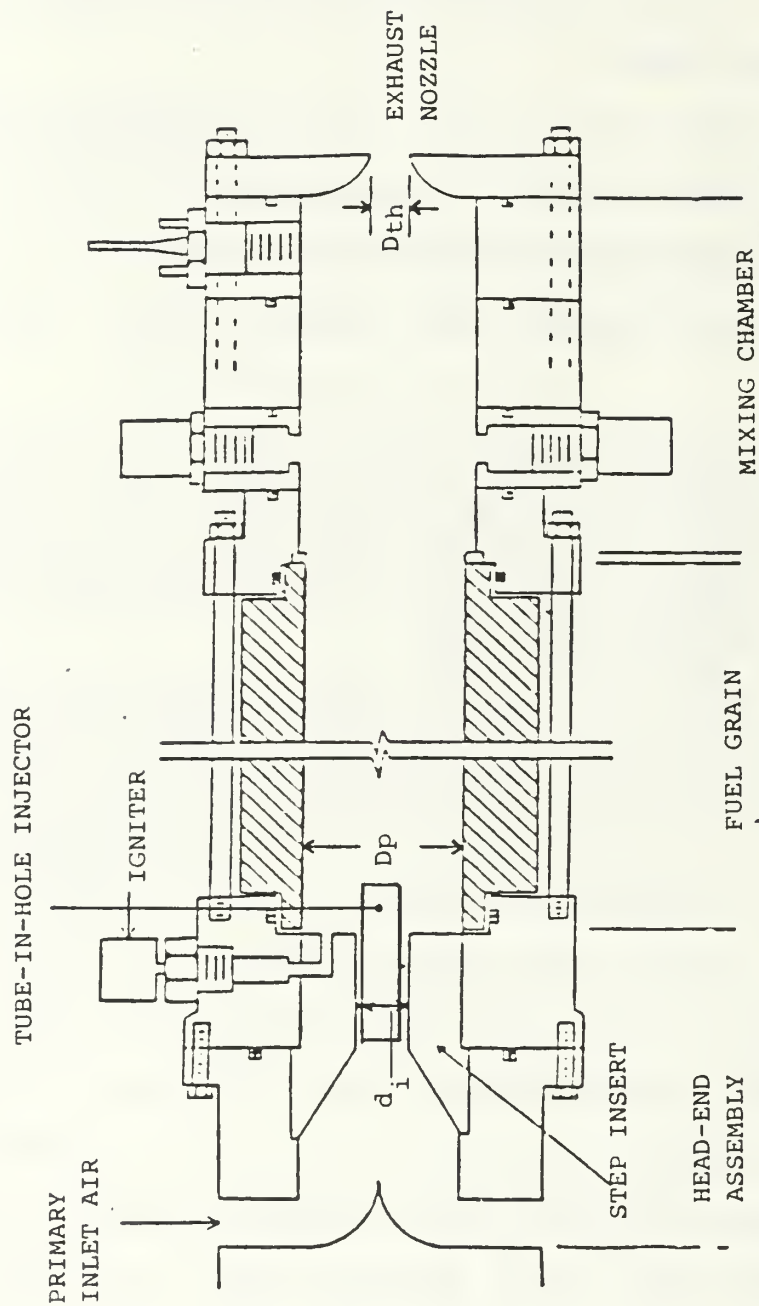
Figure 2. Depiction of Experimental SFRJ Motor Assembley

16
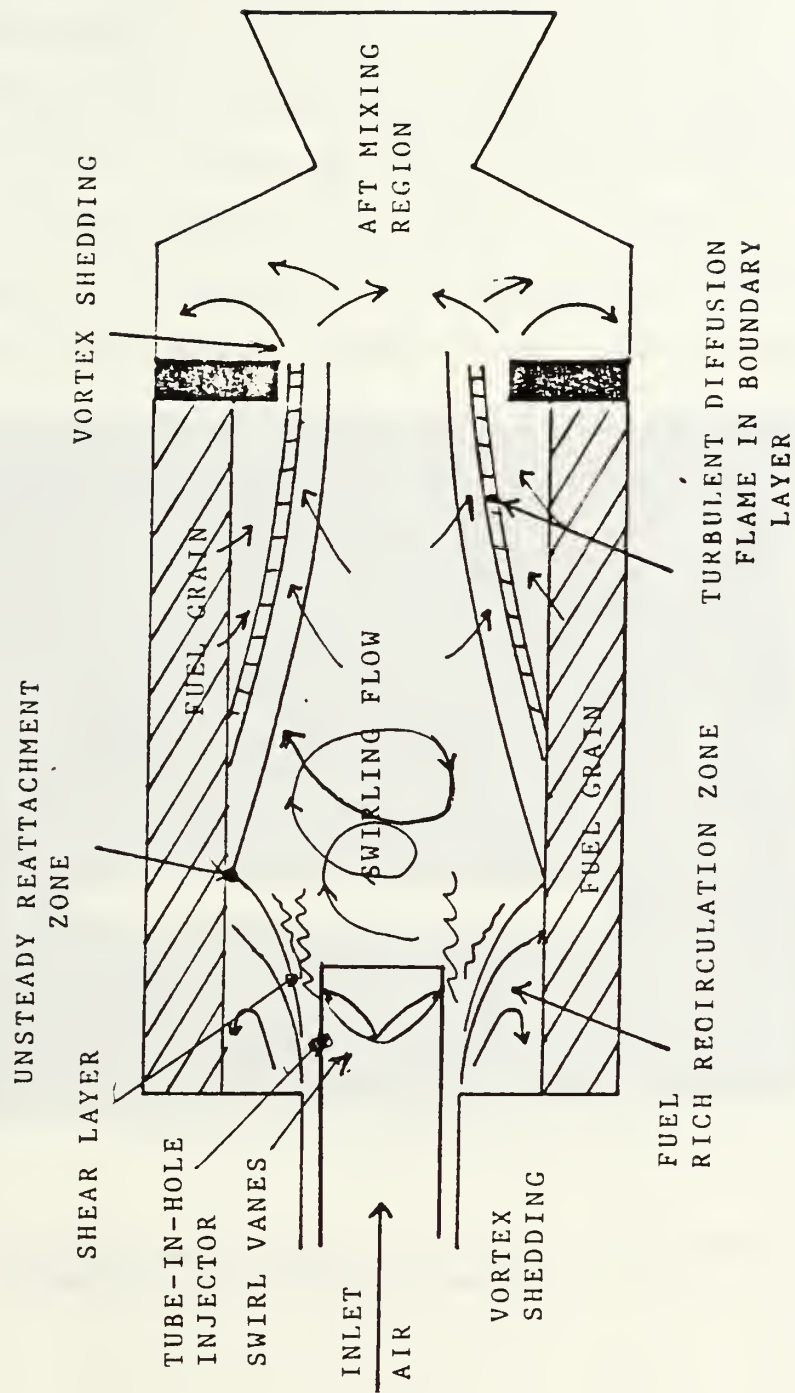
Figure 3.   Step Inlet Configuration with Tube-in-hole
            Injector

17
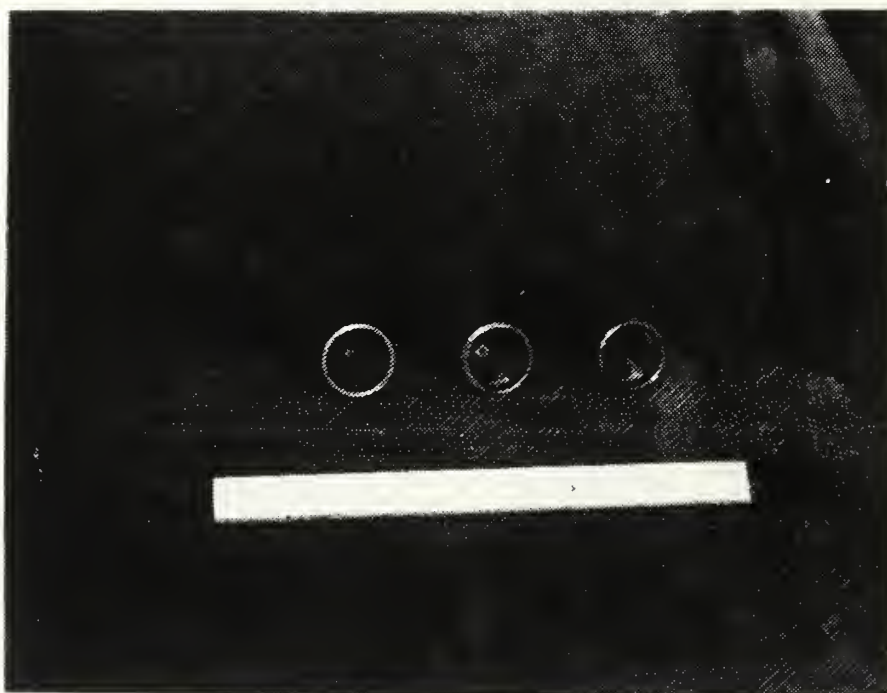
Figure 4.   15,   30,   and 45 Degree Swirl
Blades Mounted Inside Tubes

the axial centerline) swirl vane elements and a tube without a swirler were used.

CSD-18818 (an HTPB based system) was the solid fuel used for the hot runs. The average length and internal diameter of the fuel grains used were 12.0 and 1.7 inches respectively. The fuel grain was placed between the head assembly and an aft mixing chamber. The latter contained the exhaust nozzle and was connected with steel rods which bolted to the head-end assembly. The entire motor was mounted on the thrust stand. Figure 5 is a photograph of the thrust stand a the test cell. The control panel was used to initiate the runs and the Hewlett-Packard 9836 Computer and 3054A Data Acquisition/Control system sequenced events during the runs.
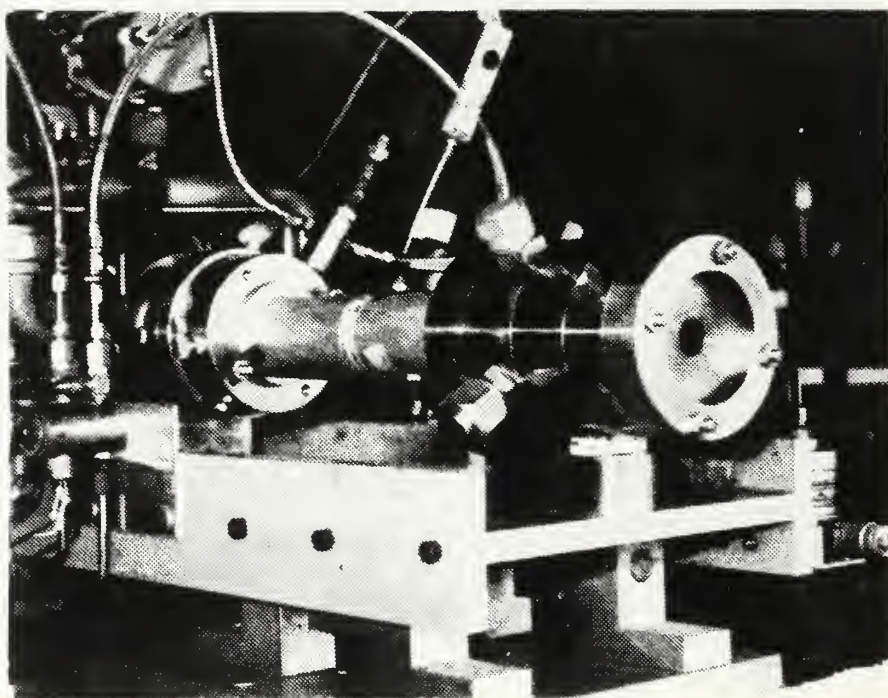
Figure 5.   Experimental Thrust Stand and SFRJ
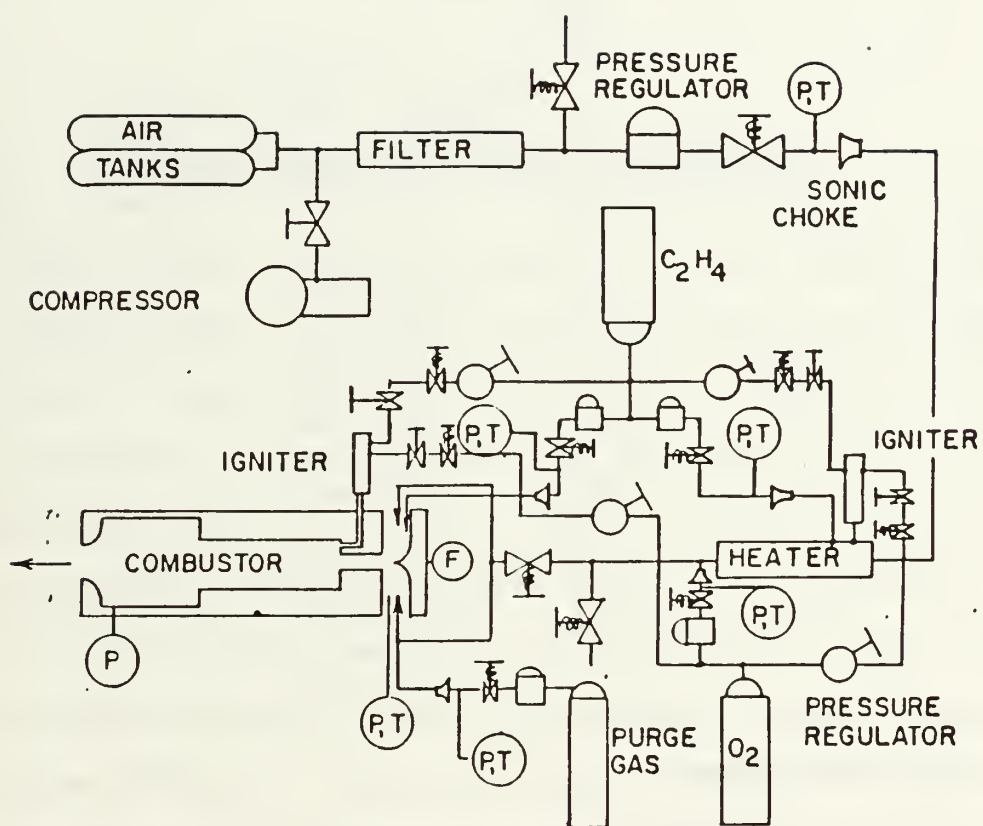
Figure 6.   Schematic of Air and Gas Supply System

21

III. EXPERIMENTAL PROCEDURES

A. CALIBRATION

Calibration of pressure transducers was conducted at the beginning of each test day utilizing a dead-weight tester. Table 1 is a list of the transducers calibrated and the calibration pressures/load.

TABLE 1

TRANSDUCER CALIBRATION PRESSURES/LOAD

Pa	500 psi
Pc	100 psi
Ph	100 psi
Phf	400 psi
Pho	500 psi
Pif	250 psi
F	100 lbf

B. DATA EXTRACTION

A Honeywell 1508B Visicorder was used to obtain analog readings from pressure and thrust transducers. Chromel-alumel thermocouples were used for measurements of all gas temperatures. A Hewlett-Packard 9836 Computer and 3054A Automatic Data Acquisition/Control Stytem were utilized to extract digital information.

C. HOT FIRING

Fuel grain length (L), average port diameter (Dp), and initial weight (W) were measured for each run. The inlet was then mounted on the ramjet motor and preparations were made for the ensuing runs.

Air and ignition gas pressures were calculated using the choked flow formula (assuming Cd = 0.97)

$$\dot{m} = \frac{C_d \; P_t \left(\frac{\pi}{4}\right) d^2 \sqrt{\gamma g_c \left(\frac{2}{\gamma+1}\right)^{\left(\frac{\gamma+1}{\gamma-1}\right)}}}{(R \; T_t)^{\frac{1}{2}}} \tag{3}$$

Pressures were set using dome loaders and mass flow rates were set using the computer system as the controlling device. The computer was then readied for data acquisiton and each test was initiated from the control panel. Table 2 lists the inlet geometry and test condintions for each run.

Upon completion of each run, the fuel grain was weighed and weight loss recorded. Actual motor burn time (tb), air time (ta), ignition time (ti), pre-ignition chamber pressure and thrust (Pa and Fa), and average chamber pressure and thrust ($\overline{Pc}$ and $\overline{F}$) were obtained from the traces recorded on the Visicorder. The change in fuel grain weight is be expressed as

$$\Delta W = \frac{\pi}{4} (\bar{d}_f^2 - \bar{d}_i^2) L \rho_f \tag{4}$$

Solving for the average final port diameter,

$$\bar{d}_f = \left(\frac{\Delta W_f \; 4}{\rho_f \; \pi L} + \bar{d}_i\right)^{\frac{1}{2}} \tag{5}$$

23

TABLE 2

INLET GEOMETRY AND TEST CONDITIONS

Run	Tube Length (in.)	Swirl Angle (deg.)	ta,ti,tb,tp (sec.)**
1	2.5	0	6,1, 6,4
2	2.5	0	6,1, 6,4
3	2.5	15	6,1, 6,4
4 *	2.5	15	6,1, 6,4
5	2.5	30	6,1, 6,4
6	2.5	30	6,1, 6,4
7	2.5	45	6,1, 6,4
8	2.5	45	6,1, 6,4

Remarks:

*   Unsuccessful first two attempts. Cooled motor,
     reweighed grain, cleaned ignition gas choke and
     torch. Third try successful.

**   pre-ignition airflow time, ignition time, burn time and
     purge time respectively

24

and substituting into

$$\bar{r} = \frac{(\bar{d}_f - \bar{d}_i)}{2\,t_b} \tag{6}$$

yeilds the average fuel regression rate.

Average values for $\dot{m}(air)$, $\dot{m}(O_2)$, $\dot{m}(C\ H_4)$, $\overline{T_i}$, and $\dot{m}(ign\ fuel)$ were then calculated from the digital printout for the run. The fuel mass flow rate was calculated by

$$\dot{m}_f = \frac{\Delta\ W_f}{t_b} \tag{7}$$

The Naval Weapons Center (NWC) China Lake, Ca., Propellant Evaluation Program (PEPCODE) was used to obtain theoretical values for the adiabatic combustion temperature and combustion gas properties, γ and R, using $\overline{Pc}$, $\overline{Ti}$, heats of formation, and elemental composition by weight of the fuel grain and injected gases used during each run. Ko [Ref. 3] gives a complete explanation of the procedures used to obtain the values needed for data reduction.

D. COLD FLOW PROCEDURES

A hemispherical, three-hole stagnation pressure probe was used to measure flow velocities at the exit plane of the tube-in-hole injector. The probe was connected by tubing to a pressure transducer. The transducer in turn, was connected through a controller to a voltmeter where stagnation pressure readings in millivolts were displayed. A Scanivalve allowed for cycling through the three pressure readings to

25

find the angle at which the flow was eminating from the tube-in-hole injector exit plane. This was accomplished by finding the maximum value for the center port and nulling the left and right values. The velocities between the tube and the inlet wall were also measured.

The probe could be rotated about its own axis. It was mounted on a vernier translation stand to allow for movement across the flow in 0.05 in. increments. The probe itself could be translated on its own axis as well as rotated. This facilitated taking measurements in the y-z plane with rotation about the y-axis. Figure 7 is a photograph of the probe mounted on the thrust stand in this configuration. With the angle of flow taken at each grid point, the probe was then rotated from the y-axis to the z-axis. Figure 8 depicts the probe head and the degrees of freedom in which it could be moved.

The pressure readings in millivolts and the angles at which the the maximum values occurred were then input into a program that caluclated x, y, and z components of the flow velocity, and transformed them from the Cartesian coordinate system to the cylindrical coordinate system. This produced axial and tangential velocity components (assuming that the net radial component was equal to zero). The computer program and examples of values calculated are given in Appendix A.
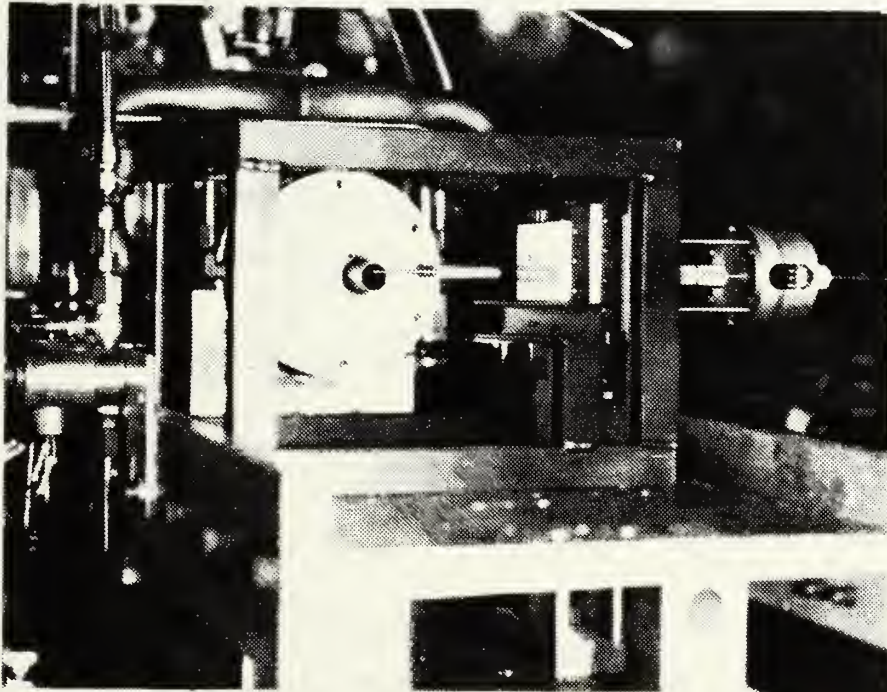
Figure 7.   Photograph of Pressure Probe on Stand
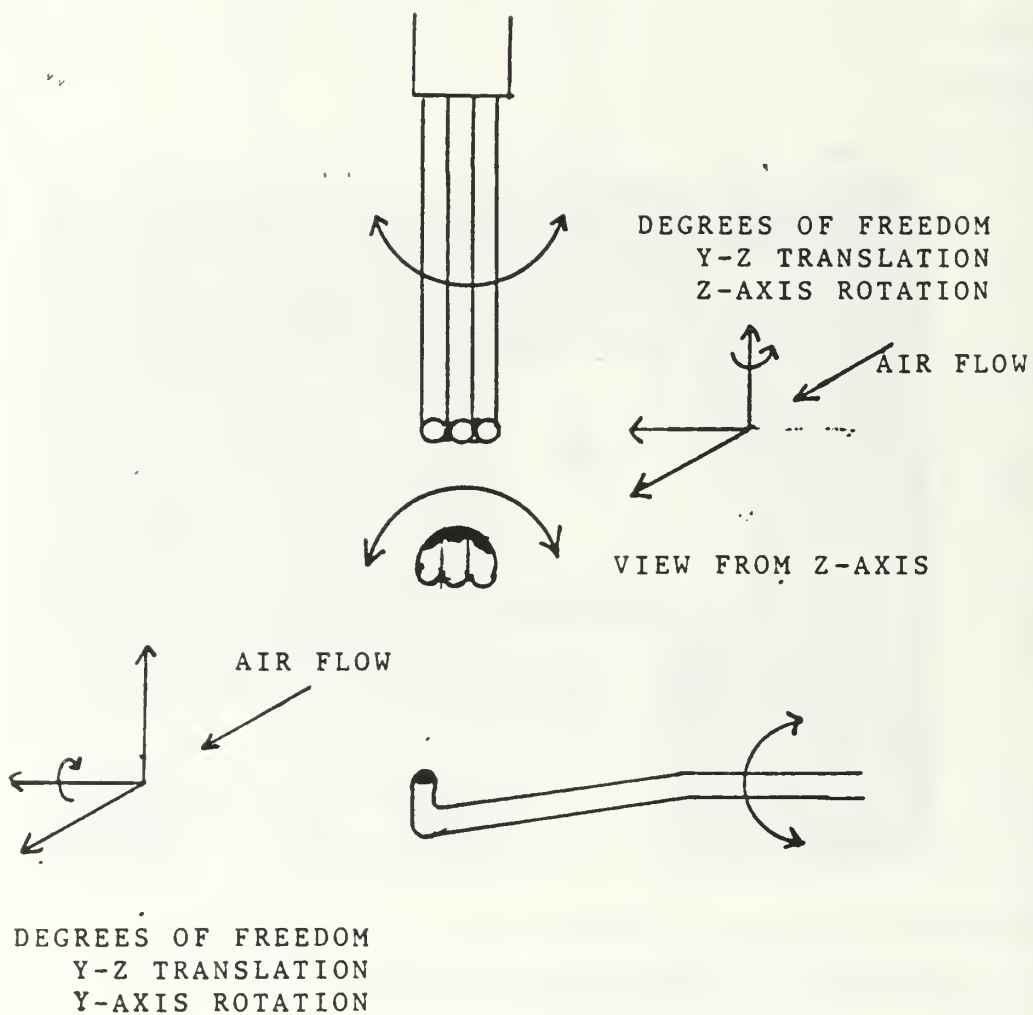
Figure 8.   Pressure Probe Head and Degrees of Freedom

Upon completion of characterization of the flow at each point in the grid, the amount of swirl in the flow was then characterized using Swirl Number (S) as previously stated in equation 2. The tangential flux of momentum is

$$G_\theta = \frac{\pi}{2} \rho \, u_o w_{mo} \, (d/2)^3 \qquad (8)$$

and the axial flux of momentum is

$$G_x = \frac{\pi}{2} \rho \, u_o \, (d/2)^2 \, (1 - (g/2)^2) \qquad (9)$$

Making the same assumptions as Lilley [Ref. 4] of solid body rotation (a flat upstream axial velocity profile, and an increasing swirl velocity from 0 at the hub to w_{mo} at the outer edge), the analysis yeilds the Swirl Number given as

$$S = \frac{G/2}{(1 - (g/2)^2)} \qquad (10)$$

where

$$G = \frac{w_{mo}}{u_{mo}} \qquad (11)$$

is the ratio of the maximum tangential velocity to axial velocity at the exit plane of the tube-in-hole injector.

In an attempt to more accurately characterize the swirl in the present apparatus, a mass averaged momentum ratio was calculated by taking the mass average tangential velocity

$$\bar{w} = \frac{\Sigma \, \dot{m} \, w}{\Sigma \, \dot{m}} \qquad (12)$$

29

and the mass average axial velocity is given by

$$\bar{u} = \frac{\Sigma \, \dot{m} \, u}{\Sigma \, \dot{m}} \tag{13}$$

Dividing equation 12 by equation 13 yeilds S(avg).

IV.   RESULTS AND DISCUSSION

A.   INITIAL TESTS

A series of initial hot runs was completed to test the integrity of the tube-in-hole injector design. During this phase it was found that initially designed tubes, which extended 0.25 inch beyond the aft end of the inlet, did not allow ignition of the motor. It was suspected that swirling flow was interferring with the recirculation zone, destroy-Ong the flame stabilization area. The tubes were lengthened so that the swirl dump was 1.5 inches beyond the inlet step, which solved the problem. This length was considerably less than the reattachment length of approximately 3.0 inches.

Burn time for the motor was initially set for 10 seconds, which almost resulted in for burn-through to the wall. Burn time was therefore reduced to 8 seconds,   which worked well for non-swirl test runs. Burn-through occurred at 8 secs. with 30 degrees of swirl,   so the burn time was further re-duced to 6 seconds and the remaining hot runs were conducted.

B.   COLD FLOW ANALYSIS

A summary of results of the cold flow studies is given in Table 3. There was an increase in the difference between the maximum and mass averaged axial velocities from 8% for no swirl, to 43% for 45 degrees of swirl. The same was true

31

for the difference between the maximum and mass averaged
tangential velocities, with 21% difference at 15 degrees and
43% difference at 45 degrees. This could have been a
function of the increased blockage within the tube. The
velocities between the tube and inlet wall increased as the
vane angle increased, which was an indication that blockage
was occurring. The Swirl number, as calculated by Equation
10 (based on solid body rotation), increased with vane angle
to 30 degrees and then decreased. The mass averaged value
(Equation 12 divided by Equation 13) increased continually
with vane angle.

TABLE 3

COLD FLOW RESULTS

Blade angle (deg)	0	15	30	45
u(max) (ft/sec)	475	616	759	820
w(max) (ft/sec)	0	309	521	525
u(avg) (ft/sec)	434	509	560	462
u(outer flow) (ft/sec)	384	393	503	589
w(avg) (ft/sec)	0	243	345	296
S(avg)	0.0	0.478	0.616	0.640
S	0.0	0.335	0.649	0.544

C. FUEL GRAIN PHYSICAL CHARACTERISTICS

The fuel grains used without swirl exhibited smooth burning surfaces with the port diameter slowly increasing to a point approximately 2.0 inches beyond the step. Thereafter, the port diameter was approximately constant. The grains used for the 15 degree swirl showed the same characteristics. However, four areas that corresponded with the four vanes of the swirl element exhibited slightly indented burn regions extending from 2 inches beyond the step to 4 inches, slowly blending into a concentric surface. The 30 degree grains showed a marked increase in the indented burn regions, and they extended to 5 inches beyond the step. The 45 degree grains were even more pronounced in the indented burned region but not as elongated. The angles of the indented burned regions corresponded to the respective swirl vane angles. Table 4 lists the physical characteristics of fuel grains pertaining to the tests.

D. COMBUSTION PROPERTIES

Measured quantities for each hot run are listed in Table 5. A plot of the regression rate vs swirl vane angle is given in Figure 9 and vs S and S(avg) in Figure 10. Regression rate increased rapidly for small amounts (15 degree vane angle) of swirl. Further increases in swirl vane angles (or Swirl Number) had much less effect on $\dot{r}$. The Swirl Number (Equation 10) correlated reasonably well with

33

regression rate. S(avg) appeared to be in question for the
45 degree vane, perhaps due to the large amount of blockage.

A typical value of G (mass flux) in an SFRJ is 0.6
lbm/in^2-sec without bypass. Fifty percent bypass would then
yeild a fuel port G of 0.3. With $\dot{r} \sim G^{.4}$, an approximately
25% reduction in $\dot{r}$ could be achieved. A 30 degree swirl, in
the present configuration, would yeild only about half of
this change in $\dot{r}$. However, it does appear that variable
swirl can be an effectiv method of regression rate control in
the SFRJ.

TABLE 4

FUEL GRAIN PHYSICAL CHARACTERISTICS

Run #	Vane Angle (deg)	L (in)	Dp (in)	Di (in)	Dth (in)	Ath (sq. in)	$\triangle$W (gm)
1	0	12.010	1.750	0.92	0.943	0.6483	197
2	0	12.000	1.749	0.92	0.943	0.6604	200
3	15	12.008	1.747	0.92	0.943	0.6554	219
4	15	12.014	1.759	0.92	0.943	0.6735	222
5	30	12.010	1.754	0.92	0.943	0.6597	233
6	30	12.060	1.740	0.92	0.943	0.6525	230
7	45	11.929	1.750	0.92	0.943	0.5721	221
8	45	11.915	1.746	0.92	0.943	0.6648	220

TABLE 5

MEASURED COMBUSTION PROPERTIES

Run#	t_i (sec)	t_b (sec)	t_a (sec)	P_a (psia)	$\dot{r}$ (in/sec)	$\overline{P_c}$ (psia)	$\overline{T_i}$ (^{0}R)
1	0.82	7.27	6.0	50.3	0.0236	100.2	1103
2	0.84	7.26	6.1	49.9	0.0240	107.8	1125
3	0.86	7.19	6.0	49.5	0.0267	105.7	1125
4	0.78	7.20	6.1	50.3	0.0266	107.8	1119
5	0.73	7.21	6.0	51.1	0.0277	108.6	1122
6	0.80	7.22	6.1	51.1	0.0274	109.3	1119
7	0.79	7.18	6.8	50.7	0.0263	107.8	1122
8	0.87	7.27	6.0	49.1	0.0276	103.8	1130

	$\dot{m}$ air (lbm/sec)	$\dot{m}$ fuel	$\dot{m}$ O_2	$\dot{m}$ CH_4	$\dot{m}$ if	$\dot{m}$ tot
1	0.503	0.0598	0.0190	0.0046	0.0033	0.593
2	0.506	0.0608	0.0190	0.0047	0.0335	0.593
3	0.495	0.0672	0.0191	0.0047	0.0034	0.589
4	0.510	0.0680	0.0193	0.0048	0.0034	0.604
5	0.508	0.0713	0.0191	0.0047	0.0034	0.606
6	0.513	0.0702	0.0194	0.0049	0.0033	0.611
7	0.503	0.0602	0.0194	0.0048	0.0034	0.591
8	0.487	0.0667	0.0192	0.0049	0.0036	0.581
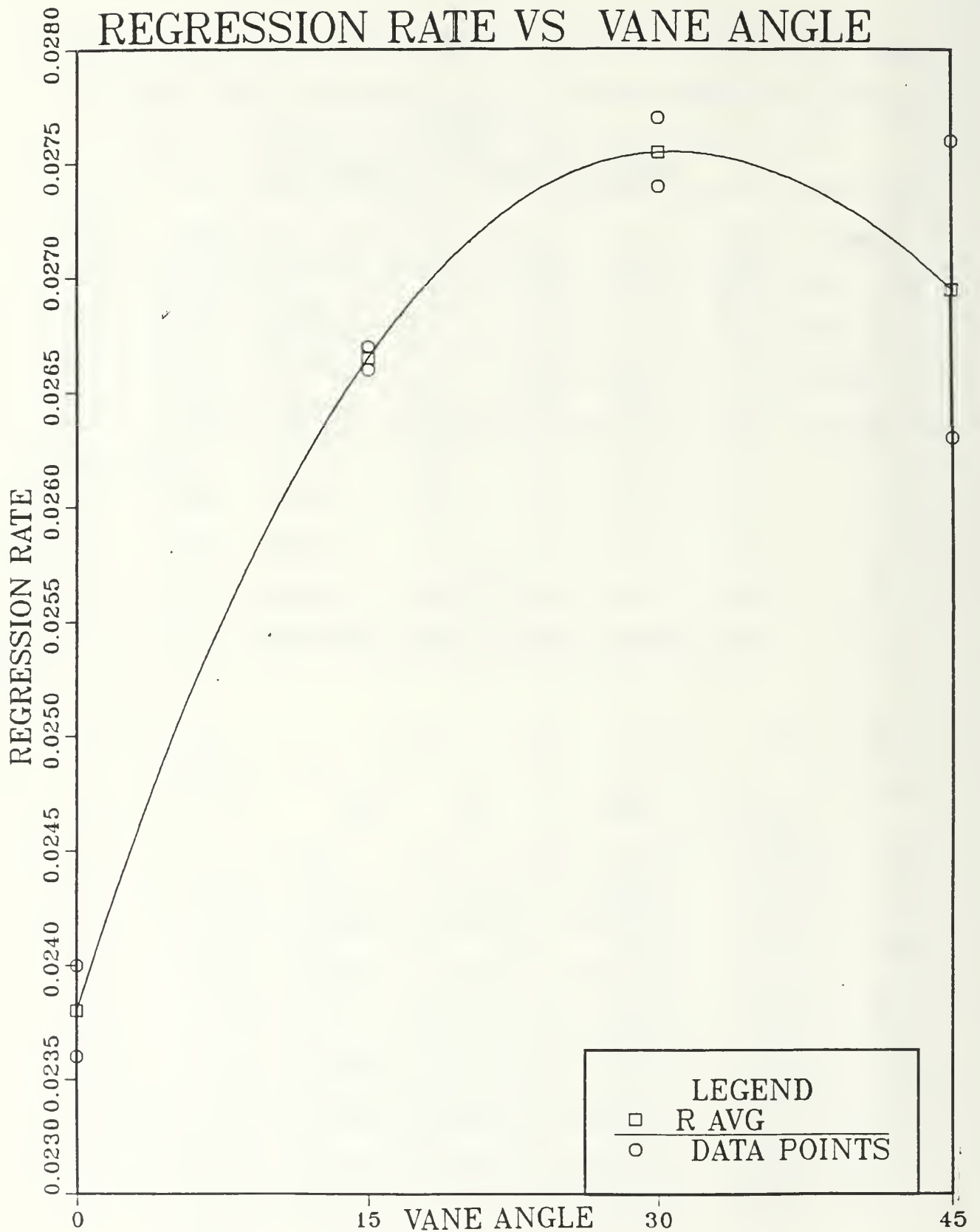
Figure 9.   Regression Rate vs. Swirl Vane Angle

REGRESSION RATE VS SWIRL NUMBER
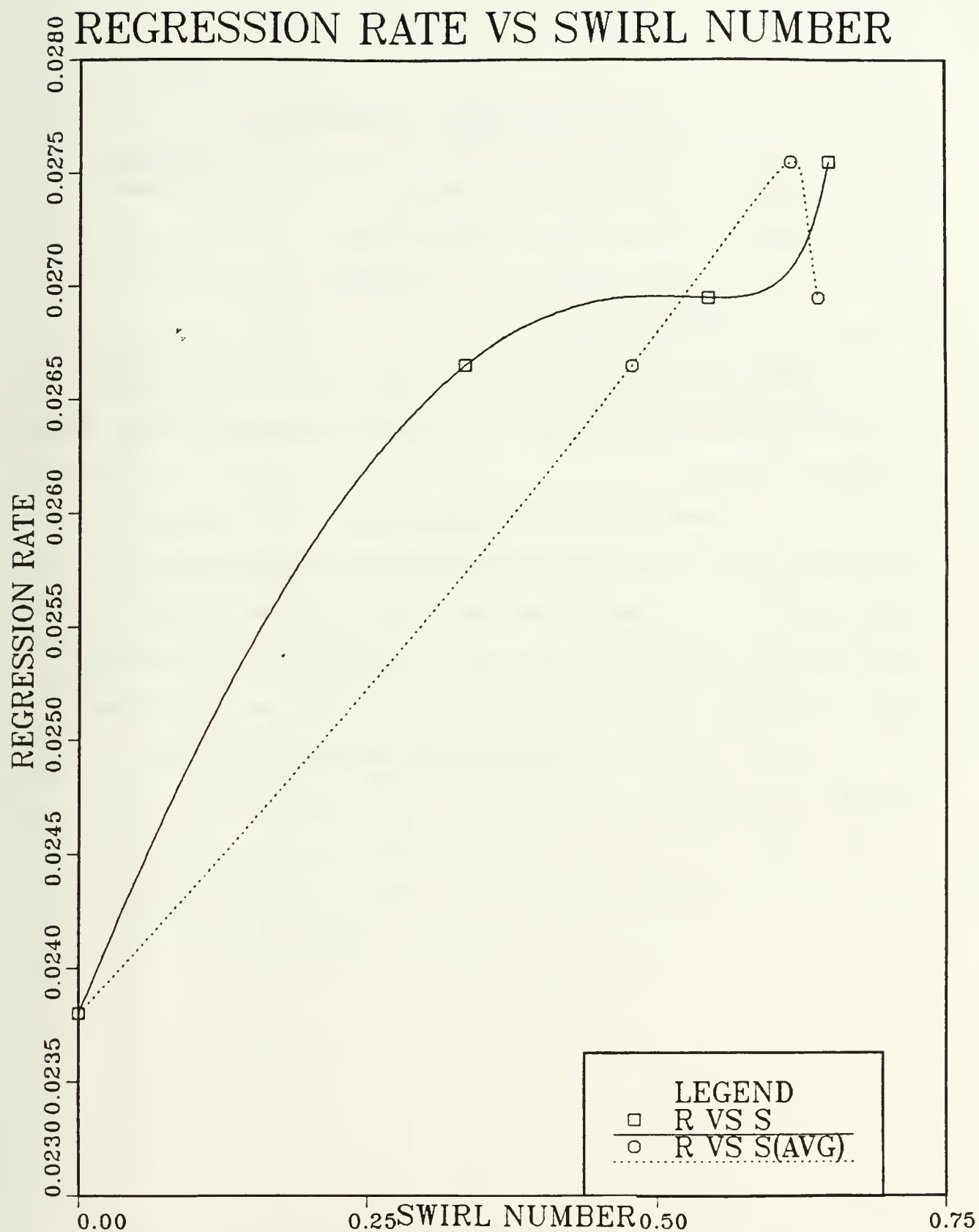
Figure 10.   Regression Rate vs Swirl Number

37

V. CONCLUSIONS AND RECOMMENDATIONS

It has been found that the regression rate increases significantly with small amounts of swirl in the flow of inlet air, but that larger amounts of swirl yield less effect. The Swirl Number S (as given by Equation 10), at the low mass flux values of approximately 0.25 which were used in this investigation, correlated reasonably well with regression rate.

It is recommended that the effects of Swirl Number on regression rate be investigated with increasing values of mass flux to 1.0 lbm/in -sec and with metalized fuels. Improvement of the 45 degree swirl element design should be also attempted, as well as an investigation of the proper-ties of combustion with swirl angles between 30 and 45 degrees and beyond.

APPENDIX A

PROGRAM FOR COLD FLOW ANALYSIS OF SWIRLING INLET AIRFLOWS

SWIRL NUMBER PROGRAM

LT. WILLIAM H. CAMPBELL, JR.

NAVAL POSTGRADUATE SCHOOL, MONTEREY

THIS PROGRAM IS USED TO COMPUTE THE AVERAGE SWIRL NUMBER OF A
SWIRLING FLOW OF A TUBE IN HOLE INJECTOR FOR A SOLID ROCKET
RAMJET AND TRANSFORM THE CARTESIAN VELOCITY COMPONENTS INTO
CYLINDRICAL VELOCITY COMPONENTS.

DEFINITIONS

TI(I)	=	INLET AIR TEMPERATURE
SONVEL(I)	=	SONIC VELOCITY
DENS(I)	=	AIR DENSITY
Y(1,K)	=	Y-CARTESIAN COORDINATE OF THE EXIT PLANE
Z(J,1)	=	Z-CARTESIAN COORDINATE OF THE EXIT PLANE
R1(J,K)	=	RADIUS TO POINT Y(N),Z(M)
RY(I,J,K)	=	PRESSURE VECTOR IN MILLIVOLTS ABOUT THE Y-AXIS
RZ(I,J,K)	=	PRESSURE VECTOR IN MILLIVOLTS ABOUT THE Z-AXIS
ALFA(I,J,K)	=	ANGLE MEASURED OF RY(N,M), POSITIVE ABOVE THE X=0
BETA(I,J,K)	=	ANGLE MEASURED OF RZ(N,M), POSITIVE LEFT OF Y=0
A1(I,J,K)	=	X COMPONENT OF RY(N,M)
A2(I,J,K)	=	X COMPONENT OF RZ(N,M)

39

```
B(I,J,K)      =   Y COMPONENT OF RZ(N,M)
C(I,J,K)      =   Z COMPONENT OF RY(N,M)
XCOMP(I,J,K)=    TOTAL X COMPONENT OF PRESSURE IN MILLIVOLTS
RTOT(I,J,K) =    TOTAL VECTOR OF PRESSURE IN MILLIVOLTS
                 IN MILLIVOLTS
RXZ(I,J,K)  =    TOTAL VECTOR COMPONENT OF PRESSURE IN THE X-Z
                 PLANE IN MILLIVOLTS
RXY(I,J,K)  =    TOTAL VECTOR COMPONENT OF PRESSURE IN THE X-Y
                 PLANE IN MILLIVOLTS
GAMMA(I,J,K)=    ANGLE BETWEEN Y=O AND RYZ
DELTA(I,J,K)=    ANGLE BETWEEN Y=O AND R1
PHI(I,J,K)  =    ANGLE BETWEEN X=O AND RXY, SWIRL ANGLE OF FLOW
TCOMP(I,J,K)=    TANGENTIAL COMPONENT OF STAGNATION PRESSURE
                 IN MILLIVOLTS
RCOMP(I,J,K)=    RADIAL COMPONENT OF STAGNATION PRESSURE IN MILLIVOLTS
PTX(I,J,K)  =    X-COMPONENT OF STAGNATION PRESSURE IN PSI
PTT(I,J,K)  =    TANGENTIAL COMPONENT OF STAGNATION PRESSURE IN PSI
U(I,J,K)    =    AXIAL VELOCITY COMPONENT
W(I,J,K)    =    TANGENTIAL VELOCITY COMPONENT
SUM1        =    SUMATION OF THE GRID REPRESENTATIVE AREA
                 MULTIPLIED BY THE GRID POINT TANGENTIAL
                 VELOCITY W(I,J,K)
SUM2        =    SUMATION OF THE GRID REPRESENTATIVE AREAS
SUM3        =    SUMATION OF THE GRID REPRESENTATIVE AREA MULT.
                 BY THE GRID POINT AXIAL VELOCITY U(I,J,K)
```

```
        UMAX(I)        =   THE MAXIMUM AXIAL VELOCITY FOR THAT RESPECTIVE
                           SWIRL VANE ANGLE
        WMAX(I)        =   THE MAXIMUM TANGENTIAL VELOCITY FOR THAT
                           RESPECTIVE SWIRL VANE ANGLE
        AW(I)          =   THE AVERAGE TANGENTIAL VELOCITY FOR THAT
                           RESPECTIVE SWIRL VANE ANGLE
        AU(I)          =   THE AVERAGE AXIAL VELOCITY FOR THAT RESPECTIVE
             ν̌            SWIRL VANE ANGLE
        SAV(I)         =   THE RATIO OF THE AW(I) TO AU(I)
        SMAX(I)        =   THE SWIRL NUMBER ACCORDING TO LILLEY ET AL
        G(I)           =   THE RATIO OF THE WMAX(I) TO UMAX(I)


   DELCARATION OF MATRICES FOR RESPECTIVE COMPONENTS OF THE PROGRAM

    REAL  Y(1,8), Z(8,1), TI(4), THETA(4), SONVEL(4), DENS(4),AW(4),
    +      RY(4,8,8), ALFA(4,8,8), RZ(4,8,8), BETA(4,8,8),AU(4),
    +      XCOMP(4,8,8), R1(8,8), RYZ(4,8,8), RTOT(4,8,8),SUM1(4),
    +      PHI(4,8,8), RCOMP(4,8,8), PTX(4,8,8), U(4,8,8), SUM2(4)
     REAL PTT(4,8,8), W(4,8,8), G(4), AREA(8,8), SUM3(4), SUM4(4),
    +      A1(4,8,8), A2(4,8,8), B(4,8,8), C(4,8,8),RXZ(4,8,8),
    +      RXY(4,8,8), DELTA(4,8,8), GAMMA(4,8,8), TCOMP(4,8,8),
    +      WMAX(4), UMAX(4), SAV(4), SMAX(4)
       INCREMENTATION OF THE Y AND Z AXIS
          DO 1 N=1,8
          READ(5,10) Y(1,N)
```

41

```
      Z(N,1)=Y(1,N)
1     CONTINUE
      DO 81 J=1,8
       READ(5,400) (AREA(J,K), K=1,8)
81    CONTINUE                          -
      COMPUTATION OF SONIC VELOCITY,DENSITY, AND INPUT OF VANE ANGLE.
      DO 2 I=1,4
       READ(5,20) TI(I), THETA(I)
       SONVEL(I)=SQRT(1.4*32.2*53.3*TI(I))
       DENS(I)=14.7/(53.3*TI(I))
2     CONTINUE


      THIS PORTION OF THE PROGRAM INPUTS AND OUTPUTS DATA RECORDED
      DURING THE COLD FLOW ANALYSIS OF DIFFERENT SWIRLER VANE
      GEOMETRIES.TH VALUE (8,8) FOR EACH ANGLE IS THE COMPONENT
      MEASURED BETWEEN THE INLET WALL AND THE TUBE-IN-HOLE INJECTOR
      OUTER WALL.


      DO 4 I=1,4
      SUM1(I)=0
      SUM2(I)=0
      SUM3(I)=0
      SUM4(I)=0
      UMAX(I)=0
```

```
      WMAX(I)=0
       DO 5 K=1,8
        DO 6 J=1,8
        READ(5,30) RY(I,J,K), ALFA(I,J,K), RZ(I,J,K), BETA(I,J,K)
          A1(I,J,K)=RY(I,J,K)*COS(ALFA(I,J,K)*3.141/180)
          A2(I,J,K)=RZ(I,J,K)*COS(BETA(I,J,K)*3.141/180)
          B(I,J,K) =RZ(I,J,K)*SIN(BETA(I,J,K)*3.141/180)
          C(I,J,K)=RY(I,J,K)*SIN(ALFA(I,J,K)*3.141/180)
          XCOMP(I,J,K)=A1(I,J,K)+A2(I,J,K)
          R1(J,K)=SQRT(Y(1,K)**2+Z(J,1)**2)
          RYZ(I,J,K)=SQRT(C(I,J,K)**2+B(I,J,K)**2)
          RXZ(I,J,K)=SQRT(C(I,J,K)**2+XCOMP(I,J,K)**2)
          RXY(I,J,K)=SQRT(XCOMP(I,J,K)**2+B(I,J,K)**2)
          RTOT(I,J,K)=SQRT(XCOMP(I,J,K)**2+B(I,J,K)**2+C(I,J,K)**2)
          IF((Y(1,K).EQ.0) .AND.(Z(J,1).EQ.0)) THEN
           DELTA(I,J,K)=0
           ELSE IF ((Z(J,1).GE.0.05) .AND. (Y(1,K).EQ.0)) THEN
           DELTA(I,J,K)=90
           ELSE
           DELTA(I,J,K)=(ATAN(Z(J,1)/Y(1,K)))*180/3.14
          END IF
          IF(B(I,J,K).EQ.0) THEN
           GAMMA(I,J,K)=0
           ELSE
           GAMMA(I,J,K)=(ATAN(C(I,J,K)/B(I,J,K)))*180/3.14
```

43

```
      END IF
      IF (XCOMP(I,J,K).EQ.0) THEN
       PHI(I,J,K)=0
        ELSE
        PHI(I,J,K)=(ATAN(B(I,J,K)/XCOMP(I,J,K)))*180/3.14
      END IF
     TCOMP(I,J,K)=RYZ(I,J,K)*COS((90-(DELTA(I,J,K)+GAMMA(I,J,K)))
    +*3.141/180)
     RCOMP(I,J,K)=RYZ(I,J,K)*SIN((90-(DELTA(I,J,K)+GAMMA(I,J,K)))
    +*3.141/180)
      PTX(I,J,K)=XCOMP(I,J,K)/.0155
     U(I,J,K)=SQRT(2402.7*TI(I)*(5*(((PTX(I,J,K)/14.7)+1)**.28571
     +1)))
      PTT(I,J,K)=TCOMP(I,J,K)/.0155
      W(I,J,K)=SQRT(2402.7*TI(I)*(5*(((PTT(I,J,K)/14.7)+1)**        .28571
    +-1)))
      SUM1(I)=SUM1(I)+(AREA(J,K)*W(I,J,K))
      SUM2(I)=SUM2(I)+AREA(J,K)
      SUM3(I)=SUM3(I)+(AREA(J,K)*U(I,J,K))
      IF (U(I,J,K).GT.UMAX(I)) THEN
       UMAX(I)=U(I,J,K)
        ELSE
        UMAX(I)=UMAX(I)
      END IF
      IF (W(I,J,K).GT.WMAX(I)) THEN
```

44

```
              WMAX(I)=W(I,J,K)
              ELSE
              WMAX(I)=WMAX(I)
            END IF
6     CONTINUE
5     CONTINUE
      AW(I)=SUM1(I)/SUM2(I)
      AU(I)=SUM3(I)/SUM2(I)
      SAV(I)=AW(I)/AU(I)
      G(I)=WMAX(I)/UMAX(I)
      SMAX(I)=(G(I)/2)/(1-G(I)**2)
4     CONTINUE
      WRITE(6,410) (UMAX(I), I=1,4)
      WRITE(6,411) (WMAX(I), I=1,4)
      WRITE(6,412) (AW(I), I=1,4)
      WRITE(6,413) (AU(I), I=1,4)
      WRITE(6,414) (SAV(I), I=1,4)
      WRITE(6,415) (SMAX(I), I=1,4)
      DO 8 I=1,4
       WRITE(6,40) THETA(I)
       WRITE(6,50) (Y(1,L), L=1,8)
       WRITE(6,55)
        DO 9 J=1,8
        WRITE(6,60) Z(J,1), (U(I,J,K),K=1,8)
9       CONTINUE
```

```fortran
3       CONTINUE
        DO 12 I=1,4
         WRITE(6,70) THETA(I)
         WRITE(6,50) (Y(1,L),L=1,8)
         WRITE(6,55)
          DO 11 J=1,8
          WRITE(6,60) Z(J,1), (W(I,J,K),K=1,8)
11        CONTINUE
12      CONTINUE
        DO 14 I=1,4
         WRITE(6,80) THETA(I)
         WRITE(6,50) (Y(1,L),L=1,8)
         WRITE(6,55)
          DO 13 J=1,8
          WRITE(6,90) Z(J,1), (RY(I,J,K), K=1,8)
13        CONTINUE
14      CONTINUE
        DO 16 I=1,4
         WRITE(6,80) THETA(I)
         WRITE(6,50) (Y(1,L),L=1,8)
         WRITE(6,55)
          DO 15 J=1,8
          WRITE(6,120) Z(J,1), (PHI(I,J,K), K=1,8)
15      CONTINUE
16      CONTINUE
```

```
       DO 18 I=1,4
         WRITE(6,100) THETA(I)
         WRITE(6,50) (Y(1,L),L=1,8)
         WRITE(6,55)
          DO 17 J=1,8
          WRITE(6,90) Z(J,1), (RZ(I,J,K), K=1,8)
17      CONTINUE
18      CONTINUE
       DO 22 I = 1,4
         WRITE(6,110) THETA(I)
         WRITE(6,50) (Y(1,L),L=1,8)
         WRITE(6,55)
          DO 21 J=1,8
          WRITE(6,120) Z(J,1), (ALFA(I,J,K), K=1,8)
21      CONTINUE
22      CONTINUE
       DO 24 I=1,4
         WRITE(6,130) THETA(I)
         WRITE(6,50) (Y(1,L), L=1,8)
         WRITE(6,55)
         DO 23 J=1,8
           WRITE(6,120) Z(J,1), (BETA(I,J,K), K=1,8)
23       CONTINUE
24      CONTINUE
       DC 32 I=1,4
```

```fortran
      WRITE(6,140) THETA(I)
      WRITE(6,50) (Y(1,L), L=1,8)
      WRITE(6,55)
       DO 31 J=1,8
       WRITE(6,150) Z(J,1), (C(I,J,K), K=1,8)
31     CONTINUE
32    CONTINUE
      DO 34 I=1,4
        WRITE(6,160) THETA(I)
        WRITE(6,50) (Y(1,L), L=1,8)
        WRITE(6,55)
        DO 33 J=1,8
         WRITE(6,150) Z(J,1), (XCOMP(I,J,K), K=1,8)
33      CONTINUE
34    CONTINUE
      DO 36 I=1,4
        WRITE(6,170) THETA(I)
        WRITE(6,50) (Y(1,L),L=1,8)
        WRITE(6,55)
         DO 35 J=1,8
         WRITE(6,150) Z(J,1), (RTOT(I,J,K), K=1,8)
35      CONTINUE
36    CONTINUE
      DO 38 I=1,4
        WRITE(6,180) THETA(I)
```

```
         WRITE(6,50) (Y(1,L), L=1,8)
         WRITE(6,55)
          DO 37 J=1,8
          WRITE(6,120) Z(J,1), (PHI(I,J,K), K=1,8)
37        CONTINUE
38     CONTINUE
       DO 42 I=1,4
         WRITE(6,190) THETA(I)
         WRITE(6,50) (Y(1,L), L=1,8)
         WRITE(6,55)
          DO 41 J=1,8
          WRITE(6,150) Z(J,1), (A1(I,J,K), K=1,8)
41        CONTINUE
42     CONTINUE
       DO 44 I=1,4
         WRITE(6,200) THETA(I)
         WRITE(6,50) (Y(1,L), L=1,8)
          WRITE(6,55)
          DO 43 J=1,8
          WRITE(6,150) Z(J,1), (A2(I,J,K), K=1,8)
43      CONTINUE
44     CONTINUE
       DO 46 I=1,4
        WRITE(6,210) THETA(I)
        WRITE(6,50) (Y(1,L), L=1,8)
```

```
          WRITE(6,55)
            DO 45 J=1,8
            WRITE(6,150) Z(J,1), (B(I,J,K), K=1,8)
45        CONTINUE
46      CONTINUE
        DO 48 I=1,4
          WRITE(6,220) THETA(I)
          WRITE(6,50) (Y(1,L), L=1,8)
          WRITE(6,55)
            DO 47 J=1,8
            WRITE(6,150) Z(J,1), (RYZ(I,J,K), K=1,8)
47        CONTINUE
48      CONTINUE
        DO 52 I=1,4
          WRITE(6,230) THETA(I)
          WRITE(6,50) (Y(1,L), L=1,8)
          WRITE(6,55)
            DO 51 J=1,8
            WRITE(6,150) Z(J,1), (RXZ(I,J,K), K=1,8)
51        CONTINUE
52      CONTINUE
        DO 54  I=1,4
          WRITE(6,240) THETA(I)
          WRITE(6,50) (Y(1,L), L=1,8)
          WRITE(6,55)
```

```
         DO 53 J=1,8
         WRITE(6,150) Z(J,1), (RXY(I,J,K), K=1,8)
53       CONTINUE
54     CONTINUE
       DO 57 I=1,4
         WRITE(6,250) THETA(I)
         WRITE(6,50) (Y(1,L), L=1,8)
         WRITE(6,55)
           DO 56 J=1,8
           WRITE(6,120) Z(J,1), (DELTA(I,J,K), K=1,8)
56       CONTINUE
57     CONTINUE
       DO 59 I=1,4
         WRITE(6,260) THETA(I)
         WRITE(6,50) (Y(1,L), L=1,8)
         WRITE(6,55)
           DO 58 J=1,8
           WRITE(6,120) Z(J,1), (GAMMA(I,J,K), K=1,8)
58       CONTINUE
59     CONTINUE
       DO 62 I=1,4
         WRITE(6,270) THETA(I)
         WRITE(6,50) (Y(1,L), L=1,8)
         WRITE(6,55)
           DO 61 J=1,8
```

```
          WRITE(6,150) Z(J,1), (TCOMP(I,J,K), K=1,8)
61        CONTINUE
62     CONTINUE
       DO 64 I=1,4
          WRITE(6,280) THETA(I)
          WRITE(6,50) (Y(1,L), L=1,8)
          WRITE(6,55)
            DO 63 J=1,8
            WRITE(6,150) Z(J,1), (RCOMP(I,J,K), K=1,8)
63        CONTINUE
64     CONTINUE
       DO 66 I=1,4
          WRITE(6,290) THETA(I)
          WRITE(6,50) (Y(1,L), L=1,8)
          WRITE(6,55)
            DO 65 J=1,8
            WRITE(6,60) Z(J,1), (PTX(I,J,K), K=1,8)
65        CONTINUE
66     CONTINUE
       DO 68 I=1,4
          WRITE(6,310) THETA(I)
          WRITE(6,50) (Y(1,L), L=1,8)
          WRITE(6,55)
            DO 67 J=1,8
            WRITE(6,60) Z(J,1), (PTT(I,J,K), K=1,8)
```

```fortran
67        CONTINUE
68      CONTINUE
        WRITE(6,330)
        WRITE(6,50) (Y(1,L), L=1,8)
        WRITE(6,55)
          DO 73 J=1,8
          WRITE(6,60) Z(J,1), (R1(J,K), K=1,8)
73        CONTINUE
10      FORMAT(F6.3)
20      FORMAT(2F6.3)
30      FORMAT(4F10.3)
40      FORMAT('1','U(I,J,K) FOR SWIRL VANE BLADE ANGLE',F5.1,'
     +.'/)
50      FORMAT(9X,'Y',8F8.3)
55      FORMAT('0',3X,'Z')
60      FORMAT(F6.3,4X,8F8.2)
70      FORMAT('1','W(I,J,K) FOR SWIRL VANE BLADE ANGLE',F5.1,'
     +.'/)
80      FORMAT('1','RY(I,J,K) FOR SWIRL VANE BLADE ANGLE',F5.1,
     +'.'/)
90      FORMAT(F6.3,4X,8F8.3)
100     FORMAT('1','RZ(I,J,K) FOR SWIRLVANE BLADE ANGLE',F5.1,'
     +.'/)
110     FORMAT('1','ALFA(I,J,K) FOR SWIRL VANE BLADE ANGLE',F5.
     +1,'.'/)
```

```
120    FORMAT(F6.3,4X,8F8.0)
130    FORMAT('1','BETA(I,J,K) FOR SWIRL VANE BLADE ANGLE',F5.
      +1,'.'/)
140    FORMAT('1','C(I,J,K) FOR SWIRL VANE BLADE ANGLE',F5.1,'
      +.'/)
150    FORMAT(F6.3,4X,8F8.3)
160    FORMAT('1','XCOMP(I,J,K) FOR SWIRL VANE BLADE ANGLE',F5
      +.1,'.'/)
170    FORMAT('1','RTOT(I,J,K) FOR SWIRL VANE BLADE ANGLE',F5.
      +1,'.'/)
180    FORMAT('1','PHI(I,J,K) FOR SWIRL VANE BLADE ANGLE',F5.1
      +,'.'/)
190    FORMAT('1','A1(I,J,K) FOR SWIRL VANE BLADE ANGLE',F5.1,
      +'.'/)
200    FORMAT('1','A2(I,J,K) FOR SWIRL VANE BLADE ANGLE',F5.1,
      +'.'/)
210    FORMAT('1','B(I,J,K) FOR SWIRL VANE BLADE ANGLE',F5.1,'
      +.'/)
220    FORMAT('1','RYZ(I,J,K) FORSWIRL VANE BLADE ANGLE',F5.1,
      +'.'/)
230    FORMAT('1','RXZ(I,J,K) FOR SWIRL VANE BLADE ANGLE',F5.1
      +,'.'/)
240    FORMAT('1','RXY(I,J,K) FOR SWIRL VANE BLADE ANGLE',F5.1
      +,'.'/)
250    FORMAT('1','DELTA(I,J,K) FOR SWIRL VANE BLADE ANGLE',F5
```

```
      +.1,'.'/)
260   FORMAT('1','GAMMA(I,J,K) FOR SWIRL VANE BLADE ANGLE',F5
      +.1,'.'/)
270   FORMAT('1','TCOMP(I,J,K) FORSWIRL VANE BLADE ANGLE',F5.
      +1,'.'/)
280   FORMAT('1','RCOMP(I,J,K) FORSWIRL VANE BLADE ANGLE',F5.
      +1,'.'/)
290   FORMAT('1','PTX(I,J,K) FOR SWIRL VANE BLADE ANGLE',F5.1
      +,'.'/)
310   FORMAT('1','PTT(I,J,K) FOR SWIRL VANE BLADE ANGLE',F5.1
      +,'.'/)
      STOP
330   FORMAT('1','R1(J,K) FOR ALL EXPERIMENTS'/)
400   FORMAT(8F8.4)
410   FORMAT('1','    UMAX(I): ',4(F6.2,',',2X))
411   FORMAT(//,'    WMAX(I): ',4(F6.2,',',2X))
412   FORMAT(//,'    AW(I): ',4(F6.2,',',2X))
413   FORMAT(//,'    AU(I): ',4(F6.2,',',2X))
414   FORMAT(//,'    SAV(I): ',4(F6.3,',',2X))
415   FORMAT(//,'    SMAX(I): ',4(F6.3,',',2X))
      END
$ENTRY
UMAX(I): 475.00,  616.81,  759.39,  820.37,

WMAX(I):  0.00,  309.46,  521.23,  525.85,
```

AW(I):   0.00,   243.41,   345.32,   296.17,

AU(I): 434.54,   509.01,   560.96,   462.46,

SAV(I): 0.000,   0.478,   0.616,   0.640,

SMAX(I): 0.000,   0.335,   0.649,   0.544,

U(I,J,K)" FOR SWIRL VANE BLADE ANGLE 15.0.

	Y	0.00	0.05	0.10	0.15	0.20	0.25	0.30	0.35
Z									
0.000		0.00	0.00	398.18	585.08	595.49	593.58	613.42	548.17
0.050		0.00	278.30	460.38	575.67	582.87	616.81	604.09	535.07
0.100		0.00	376.66	492.84	571.37	546.13	573.83	562.43	483.78
0.150		503.29	524.27	532.83	521.46	532.11	517.93	516.96	380.49
0.200		554.37	572.62	564.35	587.42	594.77	536.49	459.71	303.94
0.250		587.41	575.34	591.92	582.61	548.57	397.03	0.00	0.00
0.300		540.67	571.90	570.99	527.95	451.21	311.37	0.00	0.00
0.350		424.34	416.06	416.06	378.04	255.07	0.00	0.00	393.54

W(I,J,K) FOR SWIRL VANE BLADE ANGLE 15.0.

	Y	0.00	0.05	0.10	0.15	0.20	0.25	0.30	0.35
Z									
0.000		0.00	0.00	255.61	279.70	259.38	3.40	4.17	3.40
0.050		0.00	142.03	245.59	309.46	268.48	235.71	252.01	87.49

0.100	0.00	239.76	261.95	302.33	273.77	265.67	262.45	133.91
0.150	251.97	244.74	270.28	289.79	281.93	290.19	262.22	163.39
0.200	270.63	271.36	282.59	284.51	269.90	259.83	252.30	220.99
0.250	286.68	255.36	285.29	270.14	281.43	240.79	0.00	0.00
0.300	268.72	261.91	268.11	217.91	191.69	208.53	0.00	0.00
0.350	189.84	185.11	182.47	238.24	181.19	0.00	0.00	0.00

RY(I,J,K) FOR SWIRL VANE BLADE ANGLE 15.0.

Z \ Y	0.00	0.05	0.10	0.15	0.20	0.25	0.30	0.35
0.000	0.000	0.000	0.013	0.023	0.025	0.021	0.027	0.021
0.050	0.000	0.000	0.009	0.027	0.022	0.028	0.027	0.023
0.100	0.000	0.000	0.015	0.025	0.023	0.028	0.027	0.022
0.150	0.018	0.021	0.024	0.023	0.027	0.023	0.025	0.018
0.200	0.020	0.022	0.021	0.025	0.028	0.028	0.024	0.011
0.250	0.024	0.021	0.025	0.025	0.024	0.024	0.000	0.000
0.300	0.028	0.027	0.027	0.026	0.024	0.015	0.000	0.000
0.350	0.025	0.024	0.024	0.021	0.010	0.000	0.000	0.000

RY(I,J,K) FOR SWIRL VANE BLADE ANGLE 15.0.

Z \ Y	0.00	0.05	0.10	0.15	0.20	0.25	0.30	0.350
0.000	0.	0.	5.	5.	4.	0.	0.	0.

Z								
0.050	0.	20.	15.	8.	3.	1.	2.	0.
0.100	0.	24.	14.	8.	4.	2.	2.	0.
0.150	14.	12.	10.	9.	5.	4.	5.	0.
0.200	13.	12.	12.	9.	5.	3.	2.	3.
0.250	13.	10.	10.	8.	7.	0.	0.	0.
0.300	13.	11.	11.	7.	4.	0.	0.	0.
0.350	0.	0.	0.	0.	0.	0.	0.	0.

RZ(I,J,K) FOR SWIRLVANE BLADE ANGLE 15.0.

Y	0.00	0.05	0.10	0.15	0.20	0.25	0.30	0.35
Z								
0.000	0.000	0.000	0.012	0.028	0.027	0.030	0.028	0.022
0.050	0.000	0.011	0.023	0.023	0.028	0.027	0.026	0.018
0.100	0.000	0.021	0.021	0.024	0.021	0.020	0.019	0.012
0.150	0.020	0.019	0.018	0.018	0.015	0.012	0.014	0.004
0.200	0.025	0.026	0.026	0.026	0.024	0.014	0.007	0.004
0.250	0.027	0.027	0.027	0.025	0.021	0.000	0.000	0.000
0.300	0.016	0.021	0.021	0.014	0.005	0.000	0.000	0.000
0.350	0.000	0.000	0.000	0.000	0.000	0.000	0.000	0.021

ALFA(I,J,K) FOR SWIRL VANE BLADE ANGLE 15.0.

Y	0.00	0.05	0.10	0.15	0.20	0.25	0.30	0.35
Z								

0.000	0.	0.	42.	27.	21.	20.	20.	18.
0.050	0.	0.	34.	25.	25.	15.	18.	18.
.100	0.	0.	17.	25.	25.	20.	20.	23.
0.150	20.	3.	17.	25.	23.	24.	20.	30.
0.200	-3.	4.	12.	17.	20.	20.	23.	40.
0.250	-3.	7.	17.	19.	25.	27.	0.	0.
0.300	2.	5.	10.	10.	15.	30.	0.	0.
0.350	11.	11.	11.	23.	30.	0.	0.	0.

BETA(I,J,K) FOR SWIRL VANE BLADE ANGLE 15.0.

	Y 0.00	0.05	0.10	0.15	0.20	0.25	0.30	0.35
Z								
0.000	0.	0.	9.	8.	8.	0.	0.	0.
0.050	0.	20.	20.	16.	5.	3.	3.	0.
0.100	0.	24.	24.	15.	8.	4.	4.	0.
0.150	25.	25.	23.	20.	14.	14.	14.	0.
0.200	23.	22.	22.	18.	10.	10.	10.	10.
0.250	24.	18.	19.	15.	15.	0.	0.	0.
0.300	37.	25.	24.	20.	20.	0.	0.	0.
0.350	0.	0.	0.	0.	0.	0.	0.	0.

C(I,J,K) FOR SWIRL VANE BLADE ANGLE 15.0.

	Y 0.00	0.05	0.10	0.15	0.20	0.25	0.30	0.35

Z								
0.000	0.000	0.000	0.009	0.010	0.009	0.007	0.009	0.006
0.050	0.000	0.000	0.005	0.011	0.009	0.007	0.008	0.007
0.100	0.000	0.000	0.004	0.011	0.010	0.010	0.009	0.009
0.150	0.006	0.001	0.007	0.010	0.011	0.011	0.009	0.009
0.200	-0.001	0.002	0.004	0.007	0.010	0.010	0.009	0.007
0.250	-0.001	0.003	0.007	0.008	0.010	0.011	0.000	0.000
0.300	0.001	0.002	0.005	0.005	0.006	0.007	0.000	0.000
0.350	0.005	0.005	0.005	0.008	0.005	0.000	0.000	0.000

XCOMP(I,J,K) FOR SWIRL VANE BLADE ANGLE 15.0.

Y	0.00	0.05	0.10	0.15	0.20	0.25	0.30	0.35
Z								
0.000	0.000	0.000	0.022	0.048	0.050	0.050	0.053	0.042
0.050	0.000	0.010	0.029	0.047	0.048	0.054	0.052	0.040
0.100	0.000	0.019	0.034	0.046	0.042	0.046	0.044	0.032
0.150	0.035	0.038	0.040	0.039	0.039	0.037	0.037	0.020
0.200	0.043	0.046	0.045	0.049	0.050	0.040	0.029	0.012
0.250	0.049	0.047	0.049	0.048	0.042	0.021	0.000	0.000
0.300	0.041	0.046	0.046	0.039	0.028	0.013	0.000	0.000
0.350	0.025	0.024	0.024	0.019	0.009	0.000	0.000	0.021

RTOT(I,J,K) FOR SWIRL VANE BLADE ANGLE 15.0.

Y	0.00	0.050	0.100	0.150	0.200	0.250	0.300	0.350
Z								
0.000	0.000	0.000	0.023	0.049	0.051	0.050	0.054	0.042
0.050	0.000	0.011	0.031	0.048	0.049	0.055	0.052	0.041
0.100	0.000	0.021	0.035	0.047	0.043	0.047	0.045	0.033
0.150	0.037	0.039	0.041	0.039	0.041	0.037	0.038	0.022
0.200	0.044	0.047	0.046	0.050	0.051	0.042	0.030	0.014
0.250	0.050	0.047	0.051	0.049	0.044	0.024	0.000	0.000
0.300	0.042	0.047	0.047	0.039	0.029	0.015	0.000	0.000
0.350	0.025	0.024	0.024	0.021	0.010	0.000	0.000	0.021

PHI(I,J,K) FOR SWIRL VANE BLADE ANGLE 15.0.

Y	0.00	0.05	0.10	0.15	0.20	0.25	0.30	0.35
Z								
0.000	0.	0.	5.	5.	4.	0.	0.	0.
0.050	0.	20.	15.	3.	3.	1.	2.	0.
0.100	0.	24.	14.	8.	4.	2.	2.	0.
0.150	14.	12.	10.	9.	5.	4.	5.	0.
0.200	13.	12.	12.	9.	5.	3.	2.	3.
0.250	13.	10.	10.	8.	7.	0.	0.	0.
0.300	13.	11.	11.	7.	4.	0.	0.	0.
0.350	0.	0.	0.	0.	0.	0.	0.	0.

A1(I,J,K) FOR SWIRL VANE BLADE ANGLE 15.0.

61

Z \ Y	0.000	0.05	0.10	0.15	0.20	0.25	0.30	0.350
0.000	0.000	0.000	0.010	0.020	0.023	0.020	0.025	0.020
0.050	0.000	0.000	0.007	0.024	0.020	0.027	0.026	0.022
0.100	0.000	0.000	0.014	0.023	0.021	0.026	0.025	0.020
0.150	0.017	0.021	0.023	0.021	0.025	0.026	0.023	0.016
0.200	0.020	0.022	0.021	0.024	0.026	0.026	0.022	0.008
0.250	0.024	0.021	0.024	0.024	0.022	0.021	0.000	0.000
0.300	0.028	0.027	0.027	0.026	0.023	0.013	0.000	0.000
0.350	0.025	0.024	0.024	0.019	0.009	0.000	0.000	0.000

A2(I,J,K) FOR SWIRL VANE BLADE ANGLE 15.0.

Z \ Y	0.00	0.05	0.10	0.15	0.20	0.25	0.30	0.35
0.000	0.000	0.000	0.012	0.028	0.027	0.030	0.028	0.022
0.050	0.000	0.010	0.022	0.022	0.028	0.027	0.026	0.018
0.100	0.000	0.019	0.019	0.023	0.021	0.020	0.019	0.012
0.150	0.018	0.017	0.017	0.017	0.015	0.012	0.014	0.004
0.200	0.023	0.024	0.024	0.025	0.024	0.014	0.007	0.004
0.250	0.025	0.026	0.026	0.024	0.020	0.000	0.000	0.000
0.300	0.013	0.019	0.019	0.013	0.005	0.000	0.000	0.000
0.350	0.000	0.000	0.000	0.000	0.000	0.000	0.000	0.021

B(I,J,K) FOR SWIRL VANE BLADE ANGLE 15.0.

Z \ Y	0.00	0.05	0.10	0.15	0.20	0.25	0.30	0.35
0.000	0.000	0.000	0.002	0.004	0.004	0.000	0.000	0.000
0.050	0.000	0.004	0.008	0.006	0.002	0.001	0.001	0.000
0.100	0.000	0.009	0.009	0.006	0.003	0.001	0.001	0.000
0.150	0.008	0.008	0.007	0.006	0.004	0.003	0.003	0.000
0.200	0.010	0.010	0.010	0.008	0.004	0.002	0.001	0.001
0.250	0.011	0.008	0.009	0.006	0.005	0.000	0.000	0.000
0.300	0.010	0.009	0.009	0.005	0.002	0.000	0.000	0.000
0.350	0.000	0.000	0.000	0.000	0.000	0.000	0.000	0.000

RYZ(I,J,K) FORSWIRL VANE BLADE ANGLE 15.0.

Z \ Y	0.00	0.05	0.10	0.15	0.20	0.25	0.30	0.35
0.000	0.000	0.000	0.009	0.011	0.010	0.007	0.009	0.006
0.050	0.000	0.004	0.009	0.013	0.010	0.007	0.008	0.007
0.100	0.000	0.009	0.010	0.012	0.010	0.010	0.009	0.009
0.150	0.010	0.008	0.010	0.012	0.011	0.012	0.009	0.009
0.200	0.010	0.010	0.011	0.011	0.010	0.010	0.009	0.007
0.250	0.011	0.009	0.011	0.010	0.012	0.011	0.000	0.000
0.300	0.010	0.009	0.010	0.007	0.006	0.007	0.000	0.000
0.350	0.005	0.005	0.005	0.008	0.005	0.000	0.000	0.000

RXZ(I,J,K) FOR SWIRL VANE BLADE ANGLE 15.0.

63

Y	0.00	0.05	0.10	0.15	0.20	0.25	0.30	0.35
Z								
0.000	0.000	0.000	0.023	0.049	0.051	0.050	0.054	0.042
0.050	0.000	0.010	0.030	0.048	0.049	0.054	0.052	0.041
0.100	0.000	0.019	0.034	0.047	0.043	0.047	0.045	0.033
0.150	0.036	0.038	0.040	0.039	0.041	0.039	0.038	0.022
0.200	0.043	0.046	0.045	0.049	0.051	0.041	0.030	0.014
0.250	0.049	0.047	0.050	0.048	0.043	0.024	0.000	0.000
0.300	0.041	0.046	0.046	0.039	0.029	0.015	0.000	0.000
0.350	0.025	0.024	0.024	0.021	0.010	0.000	0.000	0.021

RXY(I,J,K) FOR SWIRL VANE BLADE ANGLE 15.0.

Y	0.00	0.05	0.10	0.15	0.20	0.25	0.30	0.35
Z								
0.000	0.000	0.000	0.022	0.048	0.050	0.050	0.053	0.042
0.050	0.000	0.011	0.030	0.047	0.048	0.054	0.052	0.040
0.100	0.000	0.021	0.035	0.046	0.042	0.046	0.044	0.032
0.150	0.036	0.039	0.040	0.038	0.040	0.037	0.037	0.020
0.200	0.044	0.047	0.046	0.049	0.050	0.040	0.029	0.012
0.250	0.050	0.047	0.050	0.048	0.042	0.021	0.000	0.000
0.300	0.042	0.047	0.047	0.039	0.028	0.013	0.000	0.000
0.350	0.025	0.024	0.024	0.019	0.009	0.000	0.000	0.021

DELTA(I,J,K) FOR SWIRL VANE BLADE ANGLE 15.0.

Y	0.00	0.05	0.10	0.15	0.20	0.25	0.30	0.35
Z								
0.000	0.	0.	0.	0.	0.	0.	0.	0.
0.050	90.	45.	27.	18.	14.	11.	9.	8.
0.100	90.	63.	45.	34.	27.	22.	18.	16.
0.150	90.	72.	56.	45.	37.	31.	27.	23.
0.200	90.	76.	63.	53.	45.	39.	34.	30.
0.250	90.	79.	68.	59.	51.	45.	40.	36.
0.300	90.	81.	72.	63.	56.	50.	45.	41.
0.350	90.	82.	74.	67.	60.	54.	49.	45.

GAMMA(I,J,K) FOR SWIRL VANE BLADE ANGLE 15.0.

Y	0.00	0.05	0.10	0.15	0.20	0.25	0.30	0.35
Z								
0.000	0.	0.	78.	70.	67.	0.	0.	0.
0.050	0.	0.	33.	61.	75.	79.	81.	0.
0.100	0.	0.	27.	60.	73.	82.	82.	0.
0.150	36.	8.	45.	58.	71.	76.	68.	0.
0.200	-6.	9.	24.	42.	67.	76.	33.	84.
0.250	-7.	17.	40.	52.	62.	0.	0.	0.
0.300	6.	15.	29.	43.	75.	0.	0.	0.
0.350	0.	0.	0.	0.	0.	0.	0.	0.

TCOMP(I,J,K) FORSWIRL VANE BLADE ANGLE 15.0.

Z \ Y	0.00	0.05	0.10	0.15	0.20	0.25	0.30	0.35
0.000	0.000	0.000	0.009	0.010	0.009	0.000	0.000	0.000
0.050	0.000	0.003	0.008	0.013	0.010	0.007	0.008	0.001
0.100	0.000	0.008	0.009	0.012	0.010	0.009	0.009	0.002
0.150	0.008	0.008	0.010	0.011	0.011	0.011	0.009	0.004
0.200	0.010	0.010	0.011	0.011	0.010	0.009	0.008	0.006
0.250	0.011	0.009	0.011	0.010	0.011	0.008	0.000	0.000
0.300	0.010	0.009	0.010	0.006	0.005	0.006	0.000	0.000
0.350	0.005	0.005	0.004	0.008	0.004	0.000	0.000	0.000

RCOMP(I,J,K) FORSWIRL VANE BLADE ANGLE 15.0.

Z \ Y	0.00	0.05	0.10	0.15	0.20	0.25	0.30	0.35
0.000	0.000	0.000	0.002	0.004	0.004	0.007	0.009	0.006
0.050	0.000	0.003	0.005	0.002	0.000	-0.000	-0.000	0.007
0.100	0.000	0.004	0.003	-0.001	-0.002	-0.002	-0.002	0.008
0.150	-0.006	0.001	-0.002	-0.003	-0.003	-0.003	-0.001	0.008
0.200	0.001	0.001	0.000	-0.001	-0.004	-0.004	-0.004	-0.003
0.250	0.001	-0.001	-0.004	-0.004	-0.005	0.008	0.000	0.000
0.300	-0.001	-0.001	-0.002	-0.002	-0.004	0.005	0.000	0.000
0.350	0.000	0.001	0.001	0.003	0.002	0.000	0.000	0.000

PTX(I,J,K) FOR SWIRL VANE BLADE ANGLE 15.0.

Y	0.00	0.05	0.10	0.15	0.20	0.25	0.30	0.35
Z								
0.000	0.00	0.00	1.39	3.11	3.23	3.21	3.44	2.71
0.050	0.00	0.67	1.88	3.01	3.09	3.48	3.33	2.57
0.100	0.00	1.24	2.16	2.96	2.69	2.98	2.86	2.08
0.150	2.26	2.46	2.55	2.44	2.54	2.40	2.39	1.26
0.200	2.77	2.97	2.88	3.14	3.22	2.59	1.87	0.80
0.250	3.14	3.00	3.19	3.08	2.71	1.38	0.00	0.00
0.300	2.63	2.96	2.95	2.50	1.80	0.84	0.00	0.00
0.350	1.58	1.52	1.52	1.25	0.56	0.00	0.00	1.35

PTT(I,J,K) FOR SWIRL VANE BLADE ANGLE 15.0.

Y	0.00	0.05	0.10	0.15	0.20	0.25	0.30	0.35
Z								
0.000	0.00	0.00	0.56	0.67	0.58	0.00	0.00	0.00
0.050	0.00	0.17	0.52	0.83	0.62	0.43	0.55	0.06
0.100	0.00	0.49	0.59	0.79	0.65	0.61	0.59	0.15
0.150	0.55	0.51	0.63	0.72	0.68	0.73	0.59	0.23
0.200	0.63	0.63	0.69	0.70	0.63	0.58	0.55	0.42
0.250	0.71	0.56	0.70	0.63	0.68	0.50	0.00	0.00
0.300	0.62	0.59	0.62	0.41	0.31	0.37	0.00	0.00

67

0.350   0.31   0.29   0.28   0.49   0.28   0.00   0.00   0.00

68

LIST OF REFERENCES

1. Chemical Systems Division, The Pocket Ramjet Reader,
    United Technologies Corporation, Sunnyvale, Ca., 1978.

2. Naval Postgraduate School, Monterey, Ca.,
    NPS-57NT73031A, An Investigation of Fuel Regression Rate
    Control in Solid Fuel Ramjets, L. D. Boaz and D. W.
    Netzer, March, 1973

3. Ko, B. N., An Experimental Investigation of Fuel
    Regression Rate Control in Solid Fuel Ramjets, Naval
    Postgraduate School, Monterey, Ca. NPS K71622

4. Oklahoma State University, Stillwater, Ok., NASA
    Contractor Report, Grant NAG3-74, An Investigation of
    Flowfields Found in Typical Combustor Geometries, D. G.
    Lilley and others, February, 1985.
    Grant NAG3-74, February, 1985.

69

INITIAL DISTRIBUTION LISTS

NO. COPIES

1. Defense Technical Information Center   2
    Cameron Station
    Alexandria, Virginia 22304-6145

2. Library, Code 0142   2
    Naval Postgraduate School
    Monterey, California 93943-5100

3. Department Charirman   1
    Department of Aeronautics, Code 67
    Naval Postgraduate School
    Monterey, California 93943-5100

4. Prof. David W. Netzer   2
    Department of Aeronautics , Code 67
    Naval Postgraduate School
    Monterey, California 93943-5100

5. Lt. William H. Campbell, Jr.   1
    814 W. Woodlawn Ave.
    Tampa, Florida 33603

6. Mrs. Roberta E. Rose   1
    846 Perrine Ct.
    Marco Island, Florida 33937